ISSN 1070-4280, Russian Journal of Organic Chemistry, 2021, Vol. 57, No. 12, pp. 1931–1939. © Pleiades Publishing, Ltd., 2021.
Russian Text © The Author(s), 2021, published in Zhurnal Organicheskoi Khimii, 2021, Vol. 57, No. 12, pp. 1706–1716.

Synthesis of Highly Functionalized Biologically Active Tetracyclic Diterpenoids from *ent*-Kaur-16-en-19-oic Acid under Modified Prévost-Woodward Reaction Conditions

O. Morarescu[a], M. Grinco[a], V. Kulcitki[a], A. Barba[a], O. Garbuz[b], A. Gulea[b], and N. Ungur[a,*]

[a] *Laboratory of Chemistry of Natural and Biologically Active Compounds, Institute of Chemistry, Chişinău, MD 2028 Moldova*

[b] *Laboratory of Advanced Materials in Biopharmaceuticals and Technics, Moldova State University, Chişinău, MD 2009 Moldova*

**e-mail: nicon.ungur@gmail.com*

Received July 15, 2021; revised July 27, 2021; accepted August 10, 2021

Abstract—A procedure has been developed for the synthesis of highly functionalized tetracyclic diterpenoids from natural *ent*-kaur-16-en-19-oic acid under modified Prévost–Woodward reaction conditions. The reaction follows an unusual pathway which leads mainly to bromination or rearrangement products. The transformation of *ent*-kaur-16-en-19-oic acid afforded a mixture of (16*ZE*)-17-bromo-*ent*-kaur-16-en-19-oic, (15*R*,16*E*)-17-bromo-15-acetoxy-*ent*-kaur-16-en-19-oic, (16*S*)-17-bromo-16-acetoxy-*ent*-kaur-19-oic, (15*S*)-15-acetoxy-*ent*-kaur-16-en-19-oic, and (15*S*)-15-hydroxy-*ent*-kaur-16-en-19-oic acids, the latter two being reported previously. The newly synthesized compounds were evaluated for their cytotoxicity against two cancer cell lines, HeLa and BxPC-3.

Keywords: *ent*-kaur-16-en-19-oic acid, diterpenoid, Prévost–Woodward reaction

DOI: 10.1134/S1070428021120058

INTRODUCTION

Terpenoids constitute the most diverse and vast class of secondary metabolites found in living organisms. Their role in natural ecosystems still remains poorly studied. The scientific communities are constantly seeking to disclose the function of each individual compound in the complex mechanism of chemical interactions at different levels, from a single cell to the entire living organism. The ultimate goal of these studies is determined by the continuously growing need for new products and materials related to health, nutrition, beauty, and other aspects of human existence.

Many terpene compounds have already found practical applications, and all of them are common chemicals. In this respect, tetracyclic *ent*-kaurane diterpenoids are appropriate subjects for study as they are widespread in plants, including cultivated ones. There is diverse interest in these compounds from the practical viewpoint. *ent*-Kauranes play a crucial role in the biosynthesis of gibberellins that are important plant growth regulators [1]. Furthermore, growing interest in *ent*-kauranes is related to prospects of their use in pharmacology. For instance, studies of plants used in folk medicine have shown that their antimicrobial, anti-inflammatory, cardiovascular, diuretic, cytotoxic, anti-HIV, and other activities are closely related to the concentration of *ent*-kauranes therein [2].

Typical sources of *ent*-kauranes are wild-growing plants in Asia and South America. Another important resource of these compounds is sunflower (*Helianthus annuus* L.) which contains a large amount of diterpenoids in all its parts, including leaves, stems, and inflorescences [3]. Sunflower is a highly available and extremely cheap source of diterpenoids, which is commercially grown throughout the world. The isolation of diterpenoids has no adverse effect on the production of sunflower oil since they are isolated from plant waste left in the fields [4]. Chemical modification of natural *ent*-kaur-16-en-19-oic acid (**1**) provides a convenient approach to hardly available biologically active diterpenoids of interest for medicinal chemistry.

The goal of the present work was to study oxidative functionalization of *ent*-kaur-16-en-19-oic acid (**1**) via Prévost–Woodward reaction under modified conditions.

RESULTS AND DISCUSSION

We previously described [5] functionalization of the C=C double bond in *ent*-kaur-16-en-19-oic acid (**1**) via peroxide epoxidation and dihydroxylation with osmium tetraoxide. Literature search for alternative olefin dihydroxylation methods has revealed Sudalai's report [6] on olefinic double bond functionalization under modified Prévost–Woodward conditions, which included a catalytic cycle based on the (diacetoxy-λ^3-iodanyl)benzene–lithium bromide couple (DIB/LiBr), as well as on the sodium periodate–lithium bromide couple ($NaIO_4$/LiBr). It should be noted that there have been no examples of the use of such approach as applied to terpene substrates.

Scheme 1 outlines the transformations of *ent*-kaur-16-en-19-oic acid (**1**) under the action of DIB/LiBr in glacial acetic acid at 95°C. The crude product was a complex mixture which was subjected to column chromatography on silica gel using gradient elution. We thus isolated 5 functionalized *ent*-kaurane derivatives, including previously unknown compounds **2**–**5**. The overall yield was 72%. The isolated compounds were as follows (in order of elution): bromides **2** and **3** (mixture of isomers, 13%), (15*R*,16*E*)-17-bromo-15-acetoxy-*ent*-kaur-16-en-19-oic acid (**4**) (40%), (16*S*)-17-bromo-16*S*-acetoxy-*ent*-kaur-19-oic acid (**5**) (17%), and previously reported [7] (15*S*)-15-acetoxy-*ent*-kaur-16-en-19-oic acid (**6**) (2%). Bromides **2** and **3** were separated by repeated silica gel column chromatography to isolate pure (16*Z*)-17-bromo-*ent*-kaur-16-en-19-oic acid (**2**) and (16*E*)-17-bromo-*ent*-kaur-16-en-19-oic acid (**3**).

The structure of acid **2** was determined on the basis of NMR data (Tables 1 and 2). Signals in the NMR spectra were assigned using two-dimensional homo- and heteronuclear experiments (HSQC, HMBC, COSY, NOESY). The ^{1}H NMR spectrum of **2** contained two methyl proton singlets at δ 1.24 and 0.95 ppm due to equatorial $C^{18}H_3$ and axial $C^{20}H_3$ groups whose orientation corresponds to the *ent*-kaur-16-en-19-oic acid (**1**) structure with the axial carboxy group (C^{19}). The other characteristic signals were those of 13-H at δ 3.02 ppm and 17-H at δ 5.81 ppm (broadened singlet).

The ^{13}C NMR spectrum of **2** showed two methyl carbon signals at δ_C 28.9 (C^{18}) and 15.6 ppm (C^{20}) and 9 methylene carbon signals (including C^{15} at δ_C 48.9 ppm). In addition, quaternary sp^3 carbon signals were observed at δ_C 43.6 (C^4), 45.2 (C^8), and 39.7 ppm (C^{10}), and the C^{16} signal appeared at δ_C 151.0 ppm. The C^{19} carbonyl carbon resonated at δ_C 183.1 ppm. The HMBC spectrum of **2** displayed correlations between 20-H and C^1, C^5, C^9, and C^{10}, between 18-H and C^3, C^4, C^5, and C^{19}, between 9-H and C^8, C^{10}, C^{11}, and C^{15}, and between 13-H and C^{12}, C^{14}, C^{15}, and C^{16} (Fig. 1), which confirmed the given assignments.

The configuration of the double C^{16}=C^{17} bond in molecule **2** was determined on the basis of the NOESY data. In particular, a correlation between 17-H and 15-H was observed, whereas no 17-H/14-H cross-peak

Scheme 1.

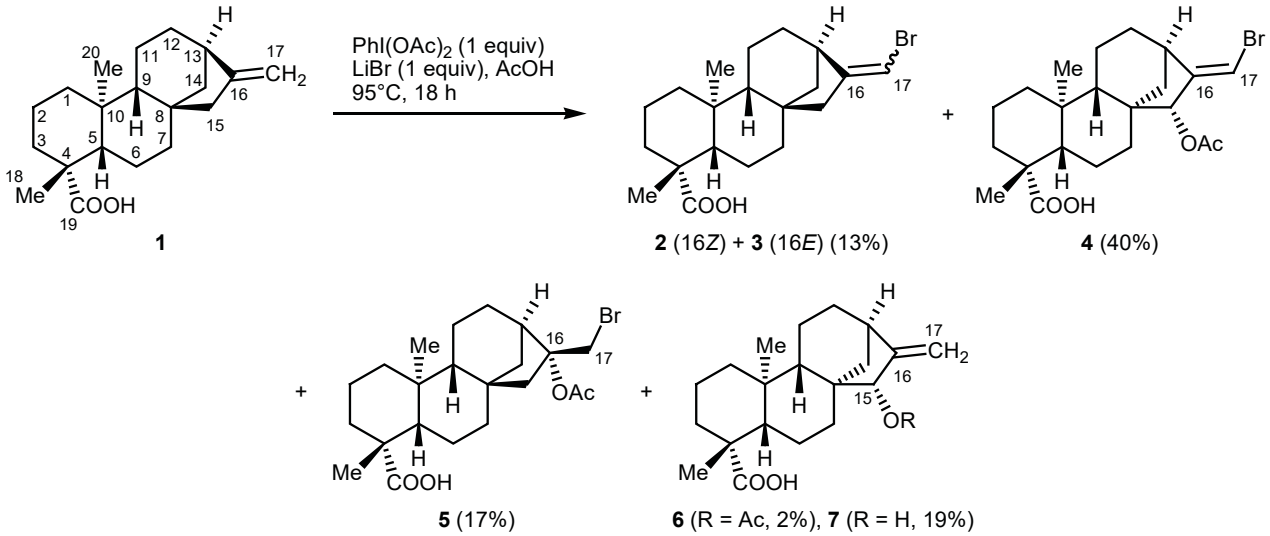


Table 1. ^{1}H NMR spectra (400 MHz) of compounds **2**–**6**

Atom no.	δ, ppm (*J*, Hz)				
	2	**3**	**4**	**5**	**6**
1	1.89 m, 0.80 m	1.87 m, 0.81 m	1.87 m, 0.81 m	1.83 m, 0.79 m	1.88 m, 0.82 m
2	1.52 m, 1.42 m	1.58 m, 1.42 m	1.85 m, 1.43 m	1.85 m, 1.45 m	1.85 m, 1.44 m
3	2.17 m, 1.0 m	2.16 m, 1.02 m	2.16 m, 1.02 m	2.15 m, 1.00 m	2.14 m, 1.00 m
4	–	–	–	–	–
5	1.04 m	1.09 m	1.09 m	1.05 m	1.08 m
6	1.84 m	1.85 m, 1.80 m	1.86 m, 1.76 m	1.82 m, 1.76 m	1.85 m, 1.76 m
7	1.51 m, 1.42 m	1.54 m, 1.50 m	1.69 m, 1.22 m	1.55 m, 1.42 m	1.64 m, 1.23 m
8	–	–	–	–	–
9	1.06 m	1.09 m	1.09 m	1.01 m	1.09 m
10	–	–	–	–	–
11	1.61 m, 1.45 m	1.85 m, 1.42 m	1.66 m, 1.43 m	1.65 m, 1.42 m	1.60 m, 1.53 m
12	1.78 m, 1.48 m	1.58 m, 1.49 m	1.77 m, 1.49 m	1.71 m, 1.50 m	1.60 m, 1.49 m
13	3.02 br.s	2.76 br.s	3.12 br.s	2.47 br.s	2.78 br.s
14	2.03 m, 1.18 m	2.08 m, 1.21 m	1.99 m, 1.51 m	1.97 m, 1.48 m	1.96 m, 1.44 m
15	2.04 m	2.11 m, 1.97 m	5.16 s	2.03 m, 1.71 m	5.26 s
16	–	–	–	–	–
17	5.81 br.s	5.87 t (2.5)	6.38 br.s	4.35 d (11.1), 3.89 d (11.1)	5.09 br.s
18	1.24 s	1.25 s	1.23 s	1.23 s	1.23 s
19	–	–	–	–	–
20	0.95 s	0.94 s	0.96 s	0.954 s	0.95 s
Me (OAc)			2.06 s	2.05 s	2.07 s

was present (Fig. 1). The 17-H proton resonated at a higher field than the corresponding proton of **3** (δ 5.81 against 5.87 ppm, respectively). The IR spectrum of **2** contained bands typical of carboxy group (1690 cm^{-1}), olefinic =C–H bond (3040 cm^{-1}), and C–Br bond (740 cm^{-1}).

Likewise, the structure of (16*E*)-17-bromo-*ent*-kaur-16-en-19-oic acid (**3**) was inferred from a similar spectroscopic data. The IR spectrum of **3** characteristically showed absorption bands due to stretching vibrations of the carboxy group (1695 cm^{-1}), =C–H bond (3030 cm^{-1}), and C–Br bond (733 cm^{-1}). In the

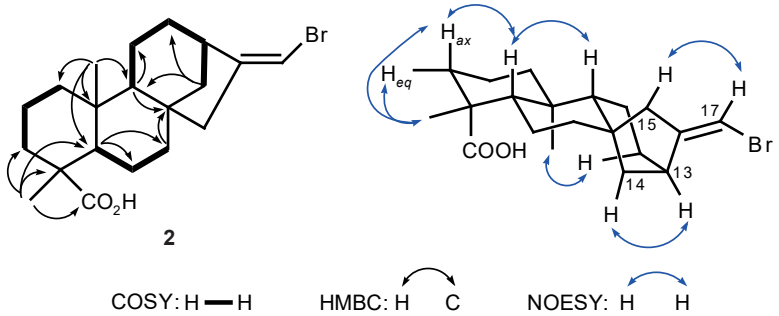


Fig. 1. Selected HMBC, COSY, and NOESY correlations for compound **2**.

Table 2. ^{13}C NMR spectra (100 MHz) of compounds **2–6**

Atom no.	δ_C, ppm				
	2	**3**	**4**	**5**	**6**
1	40.7 t	40.6 t	40.6 t	40.5 t	40.6 t
2	19.0 t	19.0 t	19.0 t	18.9 t	19.0 t
3	37.8 t	37.7 t	37.6 t	37.7 t	37.7 t
4	43.6 s	43.6 s	43.7 s	43.7 s	43.7 s
5	56.9 d	56.9 d	56.6 d	56.6 d	56.7 d
6	21.8 t	21.8 t	20.8 t	21.8 t	20.8 t
7	41.1 t	40.9 t	34.7 t	41.8 t	34.7 t
8	45.2 s	43.7 s	48.6 t	45.0 s	47.5 s
9	54.9 d	54.6 d	52.4 d	52.7 d	53.0 d
10	39.7 s	39.7 s	39.9 s	39.6 s	39.9 s
11	18.9 t	18.4 t	19.0 t	18.6 t	18.4 t
12	28.9 t	32.7 t	28.7 t	25.4 t	32.7 t
13	43.1 d	44.0 d	41.9 d	44.0 d	42.6 d
14	39.1 t	40.2 t	36.6 t	37.1 t	37.2 t
15	48.9 t	49.4 t	82.8 d	52.7 t	83.0 d
16	151.0 s	152.5 s	151.4 s	90.0 s	155.5 s
17	94.6 d	95.3 d	104.6 d	34.7 t	109.0 t
18	28.9 q	28.9 q	28.9 q	28.9 q	28.9 q
19	183.1 s	183.6 s	183.6 s	183.9 s	183.9 s
20	15.6 q	15.6 q	15.7 q	15.4 q	15.8 q
CO (OAc)			170.9 s	170.9 s	171.1 s
Me (OAc)			21.1 q	22.3 q	21.3 q

^1H NMR spectrum of **3** we observed methyl singlets at δ 1.25 and 0.94 ppm for $C^{18}H_3$ and $C^{20}H_3$, a broadened singlet at δ 2.76 ppm (13-H), and a triplet at δ 5.87 ppm (17-H, J = 2.5 Hz). The ^{13}C NMR spectrum of **3** displayed two methyl carbon signals at δ 28.9 (C^{18}) and 15.6 ppm (C^{20}) and 9 methylene carbon signals. The ^{13}C NMR spectrum confirmed the *ent*-kaurane skeleton: the quaternary sp^3-carbons resonated at δ_C 43.6 (C^4), 43.7 (C^8), and 39.7 ppm (C^{10}); the C^{16} olefinic carbon signal was observed at δ_C 152.5 ppm, and the C^{19} signal was located at δ_C 183.6 ppm. This assignment was supported by the HMBC spectrum which showed correlations of 20-H with C^1, C^5, C^9, and C^{10}, of 18-H with C^3, C^4, C^5, and C^{19}, of 9-H with C^8, C^{10}, C^{11}, and C^{15}, and of 13-H with C^{12}, C^{14}, C^{15}, and C^{16}. The spectral parameters of **3** were similar to those of isomeric bromide **2**, except for the NOESY data which clearly displayed pair correlations between 11-H, 17-H, and 13-H (Fig. 2), indicating *E* configuration of the C^{16}=C^{17} double bond.

Acid **4** contains an acetate moiety which gave rise to an ester carbonyl stretching band at 1725 cm^{-1} in the IR spectrum; in addition, bands at 1690 (COOH), 3100 (=C–H), and 730 cm^{-1} (C–Br) were present. The ^1H NMR spectrum showed signals from the equatorial $C^{18}H_3$ and axial $C^{20}H_3$ methyl groups at δ 1.23 and 0.96 ppm, respectively. The other characteristic signals were acetyl proton singlet at δ 2.06 ppm, broadened singlet of 13-H at δ 3.12 ppm, 15-H singlet at δ 5.16 ppm, and a broadened singlet at δ 6.38 ppm of 17-H. The ^{13}C NMR spectrum contained methyl carbon signals at δ_C 28.9 (C^{18}), 15.7 (C^{20}), and 21.1 ppm

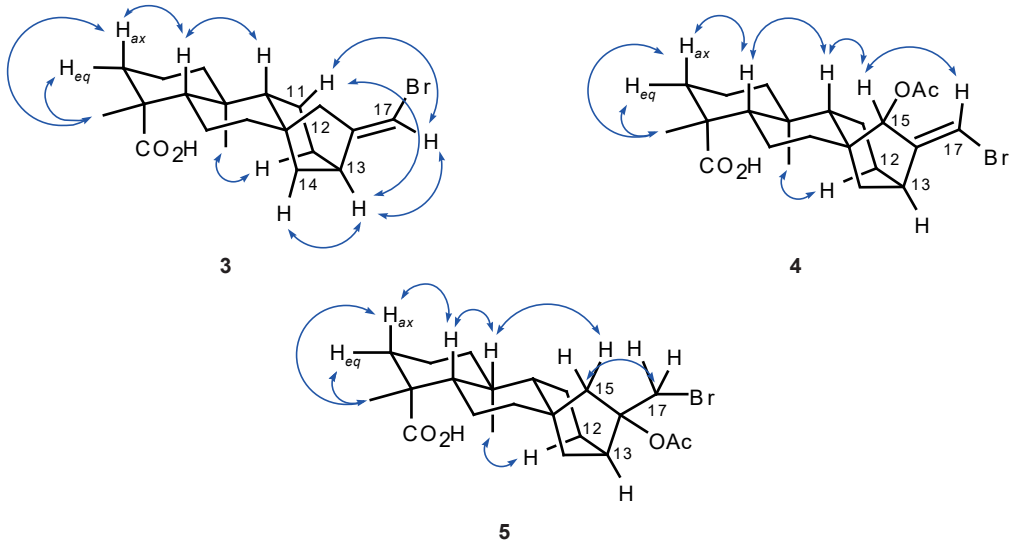


Fig. 2. Selected NOESY correlations for compounds **3**–**5**.

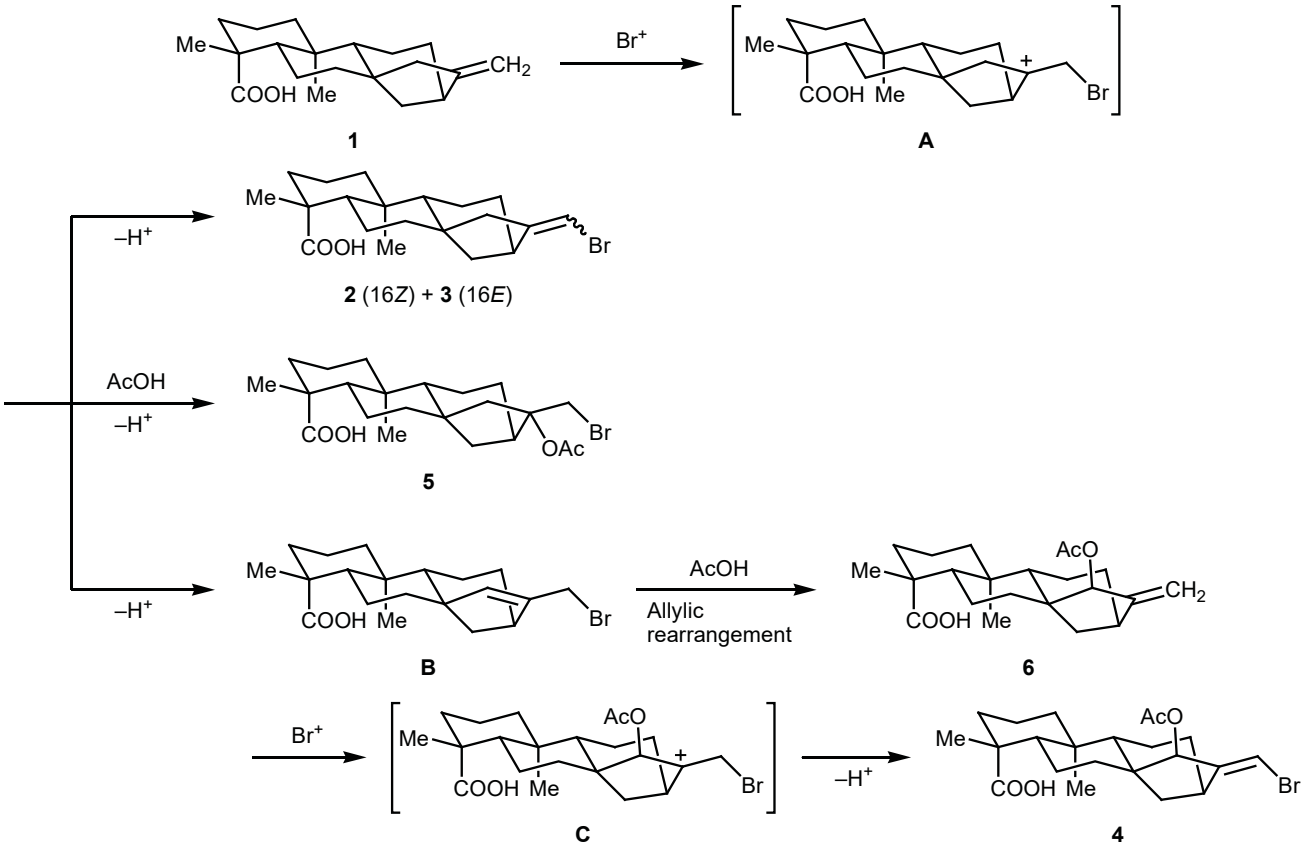
(OAc), methylene carbon signals at δ_C 40.6 (C^1), 19.0 (C^2), 37.6 (C^3), 20.8 (C^6), 34.7 (C^7), 19.0 (C^{11}), 28.7 (C^{12}), and 36.6 ppm (C^{14}), quaternary carbon signals at δ_C 43.7, 48.6, and 39.9 ppm (C^4, C^8, and C^{10}, respectively), as well as signals of the olefinic (C^{16}), acetyl carbonyl, and carboxy carbons at δ_C 151.4, 170.9, and 183.6 ppm, respectively. The HMBC correlations found for compound **4** were similar to those observed for acids **2** and **3**, but additional couplings between 15-H and acetyl carbonyl carbon (δ_C 170.9 ppm), as well as C^9, C^{13}, C^{14}, and C^{16}, were observed. The configuration at C^{15} was determined on the basis of the NOESY correlations 9-H↔15-H↔17-H and 14-H↔13-H↔12-H (Fig. 2), which indicated α-orientation of 15-H.

According to the spectral data, compound **5** is the product of addition of bromine and acetoxy group to the double bond. Its IR spectrum displayed absorption bands typical of carboxy (1690 cm^{-1}) and acetoxy groups (1717 cm^{-1}) and C–Br bond (720 cm^{-1}). The ^1H NMR spectrum showed singlets of $C^{18}H_3$ (δ 0.95 ppm), $C^{20}H_3$ (δ 1.23 ppm), and OAc groups (δ 2.05 ppm), a broadened triplet of 13-H (δ 2.47 ppm), and two doublets of $C^{17}H_2$ (δ 3.89 and 4.35 ppm, ^2J = 11.1 Hz). The ^{13}C NMR spectrum of **5** contained signals corresponding to the *ent*-kaurane skeleton, as well as additional signals of the acetate fragment (δ_C 22.3, 170.9 ppm). The C^{17} and C^{19} carbons resonated at δ_C 34.7 and 183.9 ppm, respectively. The most significant correlations observed in the HMBC spectrum of **5** are those between 20-H and C^1, C^5, C^9, and C^{10}, between 18-H and C^3, C^4, C^5, and C^{19}, between 9-H and C^8, C^{10}, C^{11}, and C^{15}, between 13-H and C^{12}, C^{14}, C^{15}, and C^{16}, and between 17-H and C^{13}, C^{15}, and C^{16}. The NOESY spectrum of **5** showed a correlation between 17-H and 15-H (Fig. 2), which indicated α-orientation of the acetoxy group on C^{16}.

The spectral characteristics of acetate **6** were identical to those reported for 15α-acetoxy-*ent*-kaur-16-en-19-oic acid [7] which is also known as acetoxy grandifloric acid. After having proved the structure of all products formed in the reaction under study, we can draw important conclusions concerning the action of modified Prévost–Woodward reagents on tetracyclic *ent*-kaurene acid **1**.

First of all, it should be noted that bifunctionalization of the double bond of **1** occurs in a quite different way than in the case of simpler substrates [6]. In fact, we succeeded in isolating only one C^{16},C^{17}-difunctional derivative, acetoxy bromide **5**, as a minor product, whereas no expected dioxygenation of the double bond was observed since the bromine atom is strongly attached to the tetracyclic skeleton. The other products, including major acetoxy bromide **4**, were formed as a result of rearrangements. This is a common outcome of cationic transformations of *ent*-cauranes, and a plausible mechanism leading to the formation of compounds **2**–**6** is shown in Scheme 2. Initial addition of bromonium ion gives carbenium ion **A** which is unlikely to undergo *anti* attack of acetate ion due to steric hindrances intrinsic to the concave tetracyclic structure. Enhanced stability of ion **A** minimizes conformational mobility of the CH_2–Br chain and favors *syn*-addition of acetate ion at the less hindered α-side of the mole-

Scheme 2.



cule, thus leading to the formation of compound **5**. On the other hand, a more preferred process is elimination of proton to give bromides **2** and **3** or hypothetical bromide **B** which adds acetate ion and is converted to products **6** and **4** as a result of allylic rearrangement.

This reaction path was confirmed by reacting *ent*-kaur-16-en-19-oic acid (**1**) with an alternative reagent system, $NaIO_4$–LiBr [6]. The product mixture contained isomeric bromides **2** and **3** (10%), (16*S*)-17-bromo-16-acetoxy-*ent*-kaur-19-oic acid (**5**) (17%), (15*S*)-15-acetoxy-*ent*-kaur-16-en-19-oic acid (**6**) (32%), and (15*S*)-15-hydroxy-*ent*-kaur-16-en-19-oic acid (**7**) (19%). Compound **7** is a natural diterpenoid occurring in many plants, and its spectral characteristics were consistent with those reported in [8].

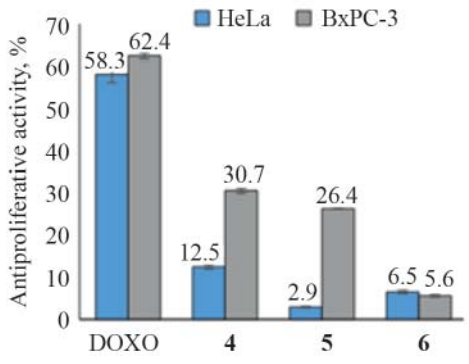


Fig. 3. Antiproliferative activity of compounds **4**–**6** and Doxorubicin (reference drug) at a concentration of 10 μM.

The antiproliferative activity of compounds **4**–**6** against HeLa epithelial cervical cancer cells and BxPC-3 human pancreatic adenocarcinoma epithelial cells was evaluated using the resazurin cytotoxicity assay which measures the number of viable cells [9]. Doxorubicin (DOXO), an anthracycline antibiotic clinically used for the treatment of a wide range of oncological diseases, was taken as reference drug. A concentration dependence was found for the inhibitory effect of the tested compounds in the micromolar range. Figure 3 compares the antiproliferative activities of compounds **4**–**6** and DOXO at a concentration of 10 μM against HeLa and BxPC-3 cancer cell lines.

The inhibitory effects of compounds **4**–**6** on HeLa and BxPC-3 cancer cell lines were lower than that of DOXO. The cytotoxic activity of **4**–**6** was estimated at $IC_{50} \geq 100$ μM; the IC_{50} values of DOXO with respect to HeLa and BxPC-3 cell lines are 2.8±0.7 and 4.0± 0.9 μM, respectively. Compounds **4**, **5**, and **6** at

a concentration of 10 μM inhibited the proliferation of cancer cells in the range of 12.5–30.7, 2.9–26.4, and 5.6–6.5%, respectively.

EXPERIMENTAL

The melting points were measured with a Boetius micro hot stage. The optical rotations were determined using a Jasco-DIP-370 polarimeter. The IR spectra were recorded on a Perkin Elmer Spectrum-100 FTIR spectrometer (UK) equipped with an ATR accessory. The ^{1}H and ^{13}C NMR spectra were recorded on a Bruker Avance-III spectrometer (Germany) at 400.13 and 100.64 MHz, respectively, using $CDCl_3$ as solvent and internal reference ($CHCl_3$, δ 7.26 ppm; $CDCl_3$, δ_C 77.0 ppm). Analytical GC/MS was performed with an Agilent 7890A chromatograph (USA) coupled with an Agilent 5975C mass-selective detector (HP-5ms capillary column, 30 m, film thickness 0.25 μm; quadrupole mass analyzer). Elemental analyses for carbon and hydrogen were carried out using a Vario-EL-III-CHNOS analyzer. Silica gel Merck 60 (70–230 mesh ASTM) was used for column chromatography. Analytical TLC was performed on Silica gel 60 F_{254} plates (Merck); spots were visualized by spraying with a 0.1% solution of cerium(IV) sulfate in 2 N sulfuric acid, followed by heating at 80°C for 5 min.

The reaction mixtures were worked-up by extraction with diethyl ether followed by washing the extract with water until neutral washings, drying over anhydrous sodium sulfate, filtering, and evaporating the solvent under reduced pressure. Commercially available reagents and solvents (Merck) were used without further purification.

Functionalization of *ent*-kaur-16-en-19-oic acid (1) by the action of $PhI(OAc)_2$/LiBr. Lithium bromide (31 mg, 0.35 mmol) was added to a solution of *ent*-kaur-16-en-19-oic acid (**1**, 106 mg, 0.35 mmol) and $PhI(OAc)_2$ (113 mg, 0.35 mmol) in glacial acetic acid (4 mL), and the mixture was stirred at 95°C for 18 h. The mixture was cooled and diluted with water (10 mL). After work-up, the crude product (113 mg) was subjected to column chromatography on silica gel (22 g; gradient elution with petroleum ether–ethyl acetate) to isolate (in order of elution) a mixture of compounds **2** and **3** (15 mg, 13%) and compounds **4**, **6**, and **5**. Isomer mixture **2**/**3** (15 mg) was separated into pure compounds **2** and **3** by repeated column chromatography on silica gel (2.0 g).

(16*Z*)-17-Bromo-*ent*-kaur-16-en-19-oic acid (2). Yield 10 mg (9%), amorphous material, $[\alpha]_D^{20}$ = –21.2° (*c* = 0.7, $CHCl_3$). IR spectrum, ν, cm^{-1}: 3030, 2937, 1690, 1258, 874, 794, 740, 635. The ^{1}H and ^{13}C NMR spectra are given in Tables 1 and 2. Found, %: C 63.00; H 7.66. $C_{20}H_{29}BrO_2$. Calculated, %: C 62.99; H 7.67.

(16*E*)-17-Bromo-*ent*-kaur-16-en-19-oic acid (3). Yield 4 mg (4%), amorphous material, $[\alpha]_D^{20}$ = –11.2° (*c* = 0.4, $CHCl_3$). IR spectrum, ν, cm^{-1}: 3040, 2943, 1695, 1258, 874, 794, 733. The ^{1}H and ^{13}C NMR spectra are given in Tables 1 and 2. Found, %: C 63.01; H 7.65. $C_{20}H_{29}BrO_2$. Calculated, %: C 62.99; H 7.67.

(15*R*,16*E*)-15-Acetoxy-17-bromo-*ent*-kaur-16-en-19-oic acid (4). Yield 45 mg (40%), amorphous material, $[\alpha]_D^{20}$ = –22.3 (*c* = 1.0, $CHCl_3$). IR spectrum, ν, cm^{-1}: 3100, 2943, 1725, 1690, 1258, 874, 794, 730. The ^{1}H and ^{13}C NMR spectra are given in Tables 1 and 2. Found, %: C 60.19; H 7.09. $C_{22}H_{31}BrO_4$. Calculated, %: C 60.14; H 7.11.

(16*S*)-16-Acetoxy-17-bromo-*ent*-kaur-19-oic acid (5). Yield 19 mg (17%), amorphous material, $[\alpha]_D^{20}$ = –73.4° (*c* = 1.0, $CHCl_3$). IR spectrum, ν, cm^{-1}: 2943, 1717, 1690, 1258, 874, 794, 720. The ^{1}H and ^{13}C NMR spectra are given in Tables 1 and 2. Found, %: C 59.81; H 7.53. $C_{22}H_{33}BrO_4$. Calculated, %: C 59.86; H 7.54.

(15*S*)-15-Acetoxy-*ent*-kaur-16-en-19-oic acid (6). Yield 2.8 mg (2%), colorless crystals, mp 172–174°C (from EtOH), $[\alpha]_D^{20}$ = –86.0° (*c* = 0.2, $CHCl_3$); published data [7]: mp 173–174°C, $[\alpha]_D^{20}$ = –84.9° (*c* = 0.15, $CHCl_3$). IR spectrum, ν, cm^{-1}: 3415–2725, 1730, 1690, 1620, 895. The ^{1}H and ^{13}C NMR spectra are given in Tables 1 and 2.

Functionalization of *ent*-kaur-16-en-19-oic acid (1) by the action of $NaIO_4$/LiBr. Lithium bromide (28 mg, 0.32 mmol), was added to a solution of *ent*-kaur-16-en-19-oic acid (**1**, 163 mg, 0.54 mmol) and $NaIO_4$ (116 mg, 0.54 mmol) in glacial acetic acid (5 mL), and the mixture was stirred at 95°C for 18 h. The mixture was cooled, diluted with water (10 mL), and worked-up as described above. The crude product (201 mg) was subjected to column chromatography on silica gel (18 g) (gradient elution, petroleum ether–ethyl acetate) to isolate (in order of elution) a mixture of compounds **2** and **3** (20 mg, 10%) and compounds **6** (64 mg, 32%), **5** (34 mg, 17%), and **7** [8] (27 mg, 19%).

Cytotoxicity evaluation of compounds 4–6. *Cell cultivation*. Human epithelial cervical cancer cells (HeLa ATCC) were cultivated in Dulbecco's modified Eagle's medium (DMEM) containing 10% fetal bovine serum (FBS), and human pancreatic adenocarcinoma epithelial cells (BxPC-3 ATCC) were in RPMI-1640

medium (Roswell Park Memorial Institute) containing 10% FBS. The cells were incubated in 25-cm^2 dishes at 37°C in a humidified 3% CO_2 atmosphere.

Resazurin proliferation assay. Resazurin is a non-fluorescent indicator dye which is reduced to pink highly fluorescent resorufin with metabolically active cells. The fluorescence intensity is proportional to the number of survived cells. Resazurin was dissolved in a saline buffer (0.9% aqueous solution of sodium chloride), and the dark blue solution was added to the cell culture in the presence of NADPH or NADH dehydrogenase as reducing agents that convert resazurin to resorufin [9].

The cells from the subconfluent cultures were trypsinized by adding trypsin–ethylenediaminetetraacetic acid (EDTA) (0.05%, 3 mL; Invitrogen) into a 50-mL centrifuge tube containing confluent cells, followed by incubation for 5 min at 37°C. The trypsin reaction was terminated by adding 10 mL of the corresponding containing 10% FBS. The cell suspension was centrifuged at 750 rpm for 10 min. The cell residue was dispersed in 2 mL of the nutrient medium containing 10% FBS, and the suspension was thoroughly stirred. The cells were counted and adjusted to a concentration of 10^{10} cells/mL. The resulting suspension was transferred to duplicated 96-well microplates (90 μL per well), and the microplates were incubated at 37°C in a 3% CO_2 atmosphere for 4 h to allow the cells to attach, and 10 μL of a solution of a tested compound was added directly to the resulting medium. The synthesized compounds were dissolved in DMSO to a concentration of 10 mM, and the obtained stock solution was then diluted to required concentration in the range 1–100 μM and incubated for 24 h. After each treatment, 20 μL of an indicator resazurin solution was added to each well, followed by incubation at 37°C in a 3% CO_2 atmosphere for 4 h. The absorbance was measured at λ 570 (D_{570}) and 600 nm (D_{600}) using a Synergy H1 Hybrid multi-detector microplate reader (BioTek). The inhibition percentage was calculated by the equation:

$$\%\text{Inhibition} = 100 - \frac{D_{570}^{\text{sample}} - D_{600}^{\text{sample}}}{D_{570}^{\text{control}} - D_{600}^{\text{control}}} \times 100.$$

CONCLUSIONS

The modified Prévost–Woodward reaction of *ent*-kaur-16-en-19-oic acid involved extended one-step functionalization with the formation of a number of compounds with the *ent*-kaurane skeleton. Unlike previously reported data on the use of this reagent system, *ent*-kaur-16-en-19-oic acid showed quite different reactivity including the addition of bromine and skeletal rearrangements. This behavior can be rationalized by steric hindrances inherent to the fused tetracyclic substrate structure, which prevent *cis*-dihydroxylation. At the same time, the *ent*-kaurane substrate under the given conditions afforded highly functionalized compounds without skeletal rearrangement. Cytotoxicity evaluation of the main reaction products revealed their moderate activity against two human cancer cell lines.

AUTHOR INFORMATION

O. Morarescu, ORCID: https://orcid.org/0000-0003-0715-8225

M. Grinco, ORCID: https://orcid.org/0000-0002-2264-2974

V. Kulcitki, ORCID: https://orcid.org/0000-0002-9363-1615

A. Barba, ORCID: https://orcid.org/0000-0002-5816-6252

O. Garbuz, ORCID: https://orcid.org/0000-0001-8783-892X

A. Gulea, ORCID: https://orcid.org/0000-0003-2010-7959

N. Ungur, ORCID: https://orcid.org/0000-0002-7457-4520

FUNDING

This study was performed under financial support by the National Research and Development Agency (ANCD) of the Moldova Republic [project nos. 20.80009.8007.03 (O.M., M.G., V.K., N.U.), 20.80009.5007.10 (O.G., A.G.), 20.80009.5007.27 (A.B.)].

CONFLICT OF INTEREST

The authors declare the absence of conflict of interest.

REFERENCES

1. Tudzynski, B., Hedden, P., Carrera, E., and Gaskin, P., *Appl. Environ. Microbiol*., 2001, vol. 67, p. 3514. https://doi.org/10.1128/AEM.67.8.3514-3522.2001
2. Ghisalberti, E.L., *Fitoterapia*, 1997, vol. 68, p. 303.
3. Pyrek, J.St., *Tetrahedron*, 1970, vol. 26, p. 5029. https://doi.org/10.1016/S0040-4020(01)93154-0

4. Ungur, N., Grinco, M., Kulcitki, V., Barba, A., Bizicci, T., and Vlad, P.F., *Chem. J. Mold*., 2008, vol. 3, p. 105. https://doi.org/10.19261/cjm.2008.03(2).01
5. Morarescu, O., Grinco, M., Kulcitki, V., Barba, A., Garbuz, O., Gudumac, V., Gulea, A., and Ungur, N., *Synth. Commun*., 2021, vol. 51, p. 123. https://doi.org/10.1080/00397911.2020.1821225
6. Emmanuvel, L., Ali Shaikh, T.M., and Sudalai, A., *Org. Lett*., 2005, vol. 7, p. 5071. https://doi.org/10.1021/ol052080n
7. Brieskorn, C.H. and Poehlmann, E., *Chem. Ber*., 1969, vol. 102, p. 2621. https://doi.org/10.1002/cber.19691020817
8. Grinco, M., Chetraru, O., Kulcitki, V., Barba, A., Boico, A., Vlad, P.F., and Ungur, N., *Chem. J. Mold*., 2010, vol. 5, p. 106. https://doi.org/10.19261/cjm.2010.05(1).11
9. Anoopkumar-Dukie, S., Carey, J.B., Conere, T., O'Sullivan, E., van Pelt, F.N., and Allshire, A., *Br. J. Radiol*., 2005, vol. 78, p. 945. https://doi.org/10.1259/bjr/54004230